Uptake and Dissolution of Gaseous Ethanol in Sulfuric Acid†

Rebecca R. Michelsen,‡,§ Sarah J. R. Staton,|| and Laura T. Iraci*

Atmospheric Chemistry and Dynamics Branch, NASA Ames Research Center, Moffett Field, California 94035-1000

Received: October 29, 2005; In Final Form: February 24, 2006

The solubility of gas-phase ethanol (ethyl alcohol, CH_3CH_2OH, EtOH) in aqueous sulfuric acid solutions was measured in a Knudsen cell reactor over ranges of temperature (209−237 K) and acid composition (39−76 wt % H_2SO_4). Ethanol is very soluble under these conditions: effective Henry's law coefficients, H^*, range from 4×10^4 M atm^{-1} in the 227 K, 39 wt % acid to greater than 10^7 M atm^{-1} in the 76 wt % acid. In 76 wt % sulfuric acid, ethanol solubility exceeds that which can be precisely determined using the Knudsen cell technique but falls in the range of 10^7-10^{10} M atm^{-1}. The equilibrium concentration of ethanol in upper tropospheric/lower stratospheric (UT/LS) sulfate particles is calculated from these measurements and compared to other small oxygenated organic compounds. Even if ethanol is a minor component in the gas phase, it may be a major constituent of the organic fraction in the particle phase. No evidence for the formation of ethyl hydrogen sulfate was found under our experimental conditions. While the protonation of ethanol does augment solubility at higher acidity, the primary reason H^* increases with acidity is an increase in the solubility of molecular (i.e., neutral) ethanol.

I. Introduction

Mixing ratios of oxygenated volatile organic compounds (OVOCs) in the remote upper troposphere are on the order of hundreds of parts per trillion by volume (pptv), for example, 850, 600, and 90 pptv for methanol, acetone, and acetaldehyde at ∼10 km, respectively.[1] With the discovery of significant amounts of organic material in acidic sulfate aerosols at altitudes above 5 km,[2] studies of the solubility and reactivity of OVOCs in cold sulfuric acid have been undertaken. For example, solubility measurements of acetone,[3−6] methanol,[7,8] and most recently, acetaldehyde,[9] have been performed under conditions that mimic sulfate particles in the upper troposphere and lower stratosphere (200−250 K, 40−70 wt % H_2SO_4). Uptake of OVOCs into aerosol particles may perturb gas-phase concentrations, the composition of the aerosol particles, and potentially the cloud nucleation properties[10] of those particles.

Ethanol has a global budget of ∼15 Tg/yr.[11] While the primary source is from biogenic emissions, anthropogenic sources are increasingly important. Use of ethanol as a fuel additive is growing in popularity since oxygenated fuels burn more cleanly, improving air quality. For example, gasoline that is composed of 10 wt % ethanol leads to a reduction of carbon monoxide emissions.[12] A competing negative result of using volatile ethanol in vehicle fuel is significant evaporative emissions, which escape before the fuel is burned. An example is evident in Brazil, where 40% of vehicle fuel is ethanol.[13] Field measurements found the mixing ratio of ethanol in Sao Paolo to be ∼170 parts per billion (ppb), 2 orders of magnitude higher than in Osaka, Japan, where no ethanol is used in fuel.[14] In the United States, the federal government has mandated an increase in ethanol use in fuel, up to 7.5 billion gallons in 2012.[15] With a lifetime due to reaction with OH (10^6 molecules cm^{-3}) of more than 3 days,[16] ethanol emitted at ground level can reach the upper troposphere. Loss via dissolution of ethanol into water droplets is not expected to be as important as gas-phase loss to OH.[1] Furthermore, convection can loft boundary layer air to the upper troposphere[17,18] and even to the stratosphere.[19] Mixing ratios of OVOCs at 10 km have been observed to double when convection over polluted areas takes place.[20] While current levels of ethanol in the remote upper troposphere are low, ∼70 pptv,[1] this amount may increase with the use of ethanol in fuel and may be significantly higher over continents when convection occurs.

The multiphase interactions between ethanol and acidic sulfate solutions under atmospheric conditions are the focus of this study. Specifically, we report measurements of ethanol solubility in low-temperature aqueous sulfuric acid solutions. The effect that protonation of the alcohol in solution has on its solubility is discussed. Ethanol is compared to other compounds, and the atmospheric implications of the suite of solubility measurements of small OVOCs studied thus far are explored. Similar to methanol,[7] no evidence for the reaction of ethanol with sulfuric acid to form ethyl hydrogen sulfate was observed, but an upper bound on the rate constant is calculated.

II. Experimental Methods

The uptake of ethanol was measured using a classic Knudsen cell apparatus,[21] which consists of two Teflon-coated Pyrex chambers separated by a valve. Pressure in the cell was measured by a capacitance manometer pressure gauge. The lower chamber was filled with several milliliters of an aqueous sulfuric acid solution of the desired concentration. Two different lower chambers were used for these experiments, each of which has two thermocouples mounted on the outside of the cell wall to measure the temperature. One chamber was suspended in a cold alcohol bath. The second lower chamber was jacketed, with cold

† Part of the special issue "David M. Golden Festschrift".

* To whom correspondence should be addressed. E-mail: Laura.T.Iraci@nasa.gov.

‡ National Research Council Associate.

§ Now at Department of Chemistry, Randolph-Macon College, Ashland, Virginia. E-mail: rmichelsen@rmc.edu.

|| Now at Department of Chemistry, Arizona State University, Tempe, Arizona.

10.1021/jp056234s CCC: $33.50
Published on Web 04/05/2006

alcohol circulated through it. For ethanol uptake experiments, the temperature of the thermocouples was calibrated once daily by measuring the vapor pressure of water above the acid solution before introduction of ethanol gas and comparing to the vapor pressure predicted by the Aerosol Inorganics Model.[22−24] These corrections were usually <1 K for the unjacketed chamber and 1−3 K for the jacketed chamber. The larger correction for the jacketed chamber is due to the location of the thermocouples in each case, either submerged in the cold bath (in cold alcohol) or on the outside of the jacket (between cold glass and air). In the case of equilibrium experiments, described below, the temperature was again calculated from the water vapor pressure, also according to the Aerosol Inorganics Model.[22−24] In this type of experiment, however, the linear relationship between the mass spectrometer signal at *m*/*z* 18 and the pressure gauge was determined at the start of the day so that the *m*/*z* 18 signal during each equilibrium experiment could be used to define the water vapor pressure. The uncertainty in the temperature measurements is estimated to be no larger than ±1 K, mostly due to an uncertainty of ∼0.1 mTorr in the water vapor pressure measurement. For the colder experiments on 76 wt % acid, the temperature uncertainty is greater, ±5 K. The water vapor pressure is so low under these conditions (<0.5 mTorr) that the 0.1 mTorr uncertainty is more significant. However, values of H^* were also very uncertain for those experiments (due to very high solubility as discussed in the Results and Discussion), hence those values of H^* are not reported or included in the thermodynamic data analysis. Thermal transpiration may be a source of systematic error in the temperature data, as discussed at the end of this section.

Gaseous water and ethanol were admitted to the upper chamber of the cell through separate capillaries and exited via one of two calibrated apertures to a differentially pumped mass spectrometer (Balzers QMG 421C electron ionization quadrupole system). The water vapor was matched to the vapor pressure of the acid to prevent changes in its composition. The total pressure in the cell was usually ≤25 mTorr to ensure that the mean free path of the gas molecules was longer than or comparable to the diameter of the escape aperture. This condition was not met for the warmest two uptake measurements over the 59 wt % acid and the warmest six measurements over the 39 wt % acid. As a result, mixing may have been hampered[21] and the true values of H^* could be somewhat higher than those observed for these few experiments.

Once stable flows of ethanol and water were established in the upper chamber of the cell, exposure to the sulfuric acid surface was initiated by opening the valve to the lower chamber. Ethanol was monitored as *m*/*z* 46 ($CH_3CH_2OH^+$); the molecular ion was used since it is free from interference by other compounds. Other fragments of ethanol (*m*/*z* 31, CH_2OH^+; *m*/*z* 45, $CH_3CH_2O^+$) were also monitored but only used in data analysis when the *m*/*z* 46 data were unavailable. Raw data from typical experiments are shown in panels a and b of Figure 1. In Figure 1a, the acid was 39 wt % H_2SO_4 and the temperature was 228 K, while in Figure 1b, the acid was colder and more concentrated (66 wt % H_2SO_4, 226 K). When exposure begins at $t = 0$ s, the gas-phase ethanol signal quickly decreases as the gas is taken up by the acid. The signal recovers slightly but does not approach its initial intensity during the duration of these experiments. The time dependence of the signal depends on the solubility and liquid-phase diffusion of ethanol in sulfuric acid (vide infra). Exposure was ended at ∼200 and 500 s in parts a and b of Figure 1, respectively, by closing the valve to the lower chamber.

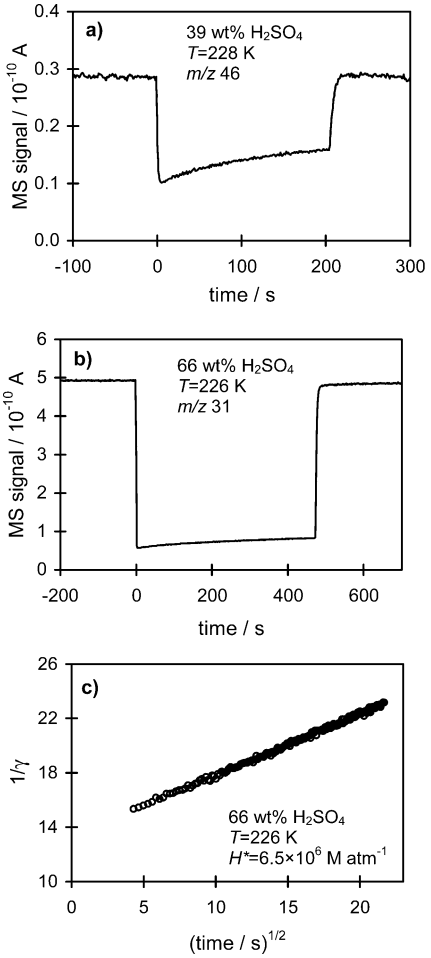

Figure 1. Uptake of gaseous ethanol by aqueous sulfuric acid. Raw data are shown in panels a and b, and analyzed data are shown in panel c. Panel c is derived from the raw data shown in panel b.

The net uptake coefficient (γ), which is defined as the fraction of incident molecules taken up by the surface, can be calculated from the raw data[21]

$$\gamma = \frac{A_h}{A_s}\left(\frac{F_O - F}{F}\right) \tag{1}$$

The number of molecules lost to the surface is measured by the change in flow to the mass spectrometer upon exposure, $F_O - F$, where F_O is the flow prior to exposure and F is the time-dependent flow during exposure. Because the mass spectrometer signal is proportional to the flow of molecules out of the cell, the signal can be used directly in the calculation. A_h is the area of the escape aperture (either 0.018 or 0.049 cm^2), and A_s is the surface area of the sulfuric acid in the cell (5.7 or 5.55 cm^2, for the unjacketed or jacketed lower chambers, respectively). The rate of ethanol diffusion into the bulk liquid, combined with the overall solubility and any reaction which occurs, controls the time dependence of γ according to[25]

$$\frac{1}{\gamma} = \frac{1}{\Gamma_g} + \frac{1}{\alpha} + \frac{\sqrt{\pi}\bar{c}}{4RTH^*\sqrt{D}}\left(\frac{1}{t^{-1/2} + \sqrt{\pi k}}\right) \tag{2}$$

where t is time, $\bar{c}$ is the average molecular velocity, R is the universal gas constant, T is the absolute temperature, D is the liquid-phase diffusion coefficient of ethanol in the solution, α is the mass accommodation coefficient, k is the pseudo-first-order rate constant for any irreversible loss (reaction), and Γ_g

TABLE 1: Measured Effective Henry's Law Coefficients for Uptake of Ethanol into Aqueous Sulfuric Acid Solutions

H_2SO_4/H_2O composition	T (K)	$H^*\sqrt{D}$ (M cm atm^{-1} s$^{-1/2}$)	D (cm^2 s^{-1})	H^* (M atm^{-1})
66.3 wt % H_2SO_4	214.4	4.18×10^3	1.47×10^{-8}	3.4×10^7
	219.0	2.47×10^3	2.57×10^{-8}	1.5×10^7
	220.8	2.33×10^3	3.15×10^{-8}	1.3×10^7
	225.7	1.49×10^3	5.20×10^{-8}	6.5×10^6
	225.8	1.19×10^3	5.25×10^{-8}	5.2×10^6
	230.0	1.02×10^3	7.65×10^{-8}	3.7×10^6
	230.1	9.05×10^2	7.71×10^{-8}	3.3×10^6
	234.1	6.71×10^2	1.07×10^{-7}	2.0×10^6
	236.7	2.45×10^2	1.31×10^{-7}	6.8×10^5
	236.8	3.29×10^2	1.32×10^{-7}	9.1×10^5
59.1 wt % H_2SO_4	208.6	1.17×10^3	2.03×10^{-8}	8.2×10^6
	218.4	1.08×10^3	5.93×10^{-8}	4.4×10^6
	218.6	9.94×10^2	6.05×10^{-8}	4.0×10^6
	218.6	7.68×10^2	6.05×10^{-8}	3.1×10^6
	223.1	3.48×10^2	9.12×10^{-8}	1.2×10^6
	229.0	2.28×10^2	1.46×10^{-7}	6.0×10^5
	230.6	2.20×10^2	1.64×10^{-7}	5.4×10^5
	230.7	2.18×10^2	1.65×10^{-7}	5.4×10^5
	236.1	1.03×10^2	2.38×10^{-7}	2.1×10^5
	237.4	9.57×10^1	2.59×10^{-7}	1.9×10^5
38.5 wt % H_2SO_4	208.7	3.82×10^2	6.43×10^{-8}	1.5×10^6
	213.5	1.22×10^2	1.07×10^{-7}	3.7×10^5
	213.7	2.07×10^2	1.10×10^{-7}	6.3×10^5
	218.9	1.24×10^2	1.77×10^{-7}	3.0×10^5
	218.9	1.76×10^2	1.77×10^{-7}	4.2×10^5
	219.4	1.25×10^2	1.86×10^{-7}	2.9×10^5
	224.7	3.49×10^1	2.84×10^{-7}	6.6×10^4
	224.9	3.49×10^1	2.88×10^{-7}	6.5×10^4
	227.2	2.93×10^1	3.44×10^{-7}	5.0×10^4
	227.3	2.07×10^1	3.46×10^{-7}	3.5×10^4
	227.6	3.47×10^1	3.54×10^{-7}	5.8×10^4
	228.1	3.42×10^1	3.67×10^{-7}	5.6×10^4

characterizes any limit due to gas-phase diffusion. In eq 2, the effective Henry's law solubility coefficient, H^*, is used, since solution-phase ethanol is not only in its molecular form, that is, a significant proportion is protonated.[26] If there is no loss due to liquid-phase reaction ($k = 0$), then plotting $1/\gamma$ vs $t^{1/2}$ yields a straight line; $H^*(D)^{1/2}$ can be calculated from the slope, and the effective Henry's law coefficient can be determined if the diffusion coefficient is known. The raw data from Figure 1b are plotted this way in Figure 1c. Diffusion coefficients were calculated according to $D = cT/\eta$, where the constant c was calculated to be 5.1×10^{-8} mol cm K^{-1} s^{-2} from the Le Bas molecular volume[27] and the viscosity of the acid, η, was calculated from the parameterization of Williams and Long.[28] The values of $H^*(D)^{1/2}$ from these uptake experiments are reported in Table 1 and are discussed in the next section.

Sulfuric acid solutions were prepared from 96 wt % stock solution (Merck) and water (Aldrich, HPLC grade). The solution concentrations were measured as 76.2 ± 0.4, 66.3 ± 0.3, 59.1 ± 0.1, 38.5 ± 0.2, and 38.4 ± 0.3 wt % H_2SO_4 by titration with 5.00 N sodium hydroxide standard (VWR). A magnetic stir bar in the acid solution allowed the sample to be mixed between uptake experiments for ≥15 min and for about 60 min in the case of equilibrium experiments described below. Gas-phase ethanol (Aldrich anhydrous 99.5%) and reagent grade water (Aldrich) were taken from the vapor above liquid samples which were purified with at least one freeze−pump−thaw cycle each day. The partial pressure of ethanol used in the experiments ranged from 0.2 to 2.3 mTorr and was <1 mTorr 75% of the time.

The measurements of H^* were independently verified by another experimental method, referred to as equilibrium experiments. Ternary solutions of sulfuric acid, water, and ethanol were mixed, and the equilibrium vapor pressure of ethanol over those solutions was measured in the jacketed Knudsen cell. This approach does not require the diffusion coefficient of ethanol in sulfuric acid to be known to calculate H^*. The mass spectral (MS) responses to water vapor (m/z 18) and ethanol (m/z 31, CH_3O^+) were calibrated with respect to the capacitance manometer measurements at the beginning of the day so that the pressure of each compound could be calculated later from the MS data. The MS response to ethanol changes slightly with the amount of water present (e.g., when the water pressure doubles, the ethanol signal decreases by 6%), presumably due to changes in the ion−molecule reactions occurring in the ionizer of the instrument. This change was accounted for by calibrating the ethanol response with approximately the correct amount of water vapor present (±3 mTorr). Error in the calculated ethanol pressure due to this effect is difficult to quantify but was usually ≤5%. Water and ethanol flows into the cell were matched to the vapor pressures over the solution, to ensure both no change in the solution composition and the measurement of true equilibrium vapor pressures. The water vapor pressure was used to calculate temperature. The measured ethanol vapor pressure, P_{EtOH}, was used to calculate H^* according to

$$H^* = [EtOH]/P_{EtOH} \quad (3)$$

Solutions were prepared by adding known amounts of ethanol to the previously mixed sulfuric acid/water solutions with a micropipet. The ethanol concentration of the solutions was constrained by the MS detection limit and varied from 0.1 M in 39 wt % to 0.8 M in 66 wt % H_2SO_4. It was assumed that the addition of small amounts of ethanol did not change the acidity of the solution since the added ethanol was always less than 5 vol % of the total solution. This assumption turned out to be incorrect in the case of the most concentrated solution, however, as discussed below. Results from these equilibrium experiments are discussed below.

Since the lower chamber of our Knudsen cell is cold, but the walls of the upper chamber are at room temperature, thermal transpiration may occur in our system. This phenomenon results in a pressure difference between two containers at different temperatures when they are connected by a hole or tube with a sufficiently small diameter. The magnitude of this effect depends on the Knudsen number, $Kn = \lambda/d$, where λ is the mean free path of the gas and d is the diameter of the hole. When Kn is much less than one, hydrodynamic conditions prevail, and the pressures in the hot container and the cold container are equal: $P_2/P_1 = 1$. However, if Kn is much greater than one, then molecular flow conditions exist and the ratio of the pressures is equal to the square root of the ratio of the temperatures: $P_2/P_1 = (T_2/T_1)^{1/2}$.[29−31]

Accurate measurement of pressure is crucial for all temperature calibrations described previously, as they rely on the water vapor pressure. The equilibrium solubility experiments require careful determination of the ethanol pressure (eq 3), but the quantity measured by the uptake method, $H^*(D)^{1/2}$, is not affected. We considered the potential influence of thermal transpiration on two aspects of our system: (1) the temperature difference between the Knudsen cell (298 K) and the head of the capacitance manometer (318 K), which are connected by tubing of $d \approx 5$ mm, and (2) the difference between the cold lower chamber (<240 K) and the upper chamber of the Knudsen cell, which are joined at their narrowest point by an opening of $d \approx 2.7$ cm. We evaluated Kn for both situations over our range of experimental conditions and found it was almost always in the intermediate region around unity ($0.04 \leq Kn \leq 12$). Thus, the real correction factor for pressure measured in our Knudsen cell

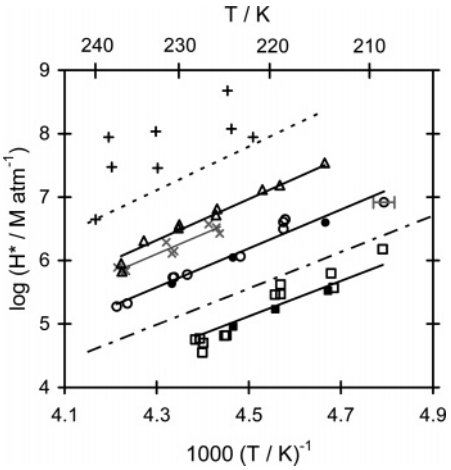

Figure 2. Summary of measurements of ethanol solubility in sulfuric acid as a function of temperature. Uptake and equilibrium experiments are shown as open and closed symbols, respectively: squares for 39 wt %, circles for 59 wt %, and triangles for 66 wt % H_2SO_4. The solubility of ethanol in water[33] is shown as a dashed−dotted line. The lower limits of solubility in 76 wt % H_2SO_4 are shown as plus signs (+). Equilibrium experiments for the 0.8 M EtOH, 66 wt % H_2SO_4 ternary solution are shown as gray crosses (×). Representative temperature error bars are included on the coldest 59 wt % data point. Error bars on H^* are about the size of the symbols. See text for discussion.

TABLE 2: Thermodynamic Parameters for Ethanol Dissolution in Aqueous Sulfuric Acid

H_2SO_4/H_2O composition	$x_{H_2SO_4}$	M_{solv}[a] (mol L^{-1})	$\Delta H°$ (kJ mol^{-1})	$\Delta S°$ (J mol^{-1} K^{-1})
0 wt % H_2SO_4	0.00	55.6	−54.8	−174
38.5 wt % H_2SO_4	0.10	46.0	−69.6	−247
59.1 wt % H_2SO_4	0.21	35.3	−58.3	−173
66.3 wt % H_2SO_4	0.27	30.7	−68.2	−201
38.5 wt % H_2SO_4	0.10	46.0	−53.3	−174
59.1 wt % H_2SO_4	0.21	35.3	−58.4	−174
66.3 wt % H_2SO_4	0.27	30.7	−61.9	−174

[a] Calculated at 220 K.

may well lie between unity and the molecular-flow limit $(T_2/T_1)^{1/2}$ (∼0.9).

While no theoretical or semiempirical equation is capable of quantitatively predicting thermal transpiration effects in the intermediate region,[31] we can calculate a bound for the possible correction of greatest magnitude. Since the temperature difference between the cell and the capacitance manometer is small, the error in pressure measurement due to this effect could be at most 2−3%. The temperature difference between the cold acid and the room-temperature Knudsen cell is larger, and therefore the effect of thermal transpiration may be more pronounced. The average maximum correction to the temperature of all the experiments is -1.1 ± 0.1 (1σ) K. In the case of the uptake experiments, a lower temperature leads to a smaller diffusion coefficient, which increases the value of H^*. For the maximum correction, values of H^* increase on average by 6%, which is significantly less than the overall error in H^* (∼15−30% as discussed in the next section). In the case of equilibrium experiments, the maximum correction to the pressure results in a decrease of 11−16%, which is equivalent to an increase of 12−19% in H^*.

For both types of experiments, the corrections to temperature and H^* nearly counter each other so that the calculated thermodynamic parameters (see Figure 2 and Table 2) change by less than 1%. Given the magnitude of other uncertainties in our H^* values and temperature measurements, coupled with the lack of a definitive correction for this effect in the transition regime, we recommend using the uncorrected values presented here. Systematic errors introduced by ignoring thermal transpiration effects are believed to be less than 20% in H^* values and are nearly insignificant for the thermodynamic parameters derived. For completeness, we have provided all the maximally corrected values in the Supporting Information.

III. Results and Discussion

Ethanol uptake experiments were performed in the Knudsen cell over ranges of acid composition (39−76 wt % H_2SO_4) and temperature (209−237 K). The raw data for two different experiments are shown in panels a and b of Figure 1. In Figure 1a, the experimental conditions were 228 K, 39 wt % H_2SO_4, while in 1b the 66 wt % acid was maintained at 226 K. The larger uptake of ethanol in the 66 wt % acid (panel b) vs the 39 wt % acid (panel a) is exhibited by both the percentage the gas-phase ethanol signal drops at $t = 0$ s and the amount of recovery during exposure.

The raw data for each experiment were analyzed by the method outlined above; the uptake coefficient was calculated from the ethanol signal (eq 1), and its inverse was plotted vs square root of time. The Henry's law coefficient was determined from the slope according to eq 2 with $k = 0$. For example, the raw data shown in Figure 1b were analyzed and plotted (Figure 1c) resulting in $H^* = 6.5 \times 10^6$ M atm^{-1}. The data at $t^{1/2} < 4.8$ s$^{1/2}$ were not included in the analysis because eq 2 does not reproduce the coupled differential equations which describe the uptake processes soon after the valve is opened[32] and because during blank experiments (no acid in the cell, but cold walls) some initial wall loss of ethanol was observed at $t < 23$ s.

A summary of the measurements of the solubility of ethanol in low-temperature sulfuric acid is given in Table 1, along with experimental conditions and the calculated D values. The main sources of uncertainty in H^* are the uncertainty in the diffusion coefficient, commonly ∼10% but up to 30% for the most viscous solutions, and the error in determining the slope of the $1/\gamma$ data. The error inherent in data analysis (e.g., due to instability in the delivered flow of ethanol) was usually ≤12%. Thus, the overall uncertainty in H^* is usually ∼15% but larger for the more concentrated, colder acid solutions. The measured Henry's law coefficients determined from the time-dependent uptake experiments are plotted in Figure 2 as open symbols: □ for 39 wt %, ○ for 59 wt %, and △ for 66 wt % H_2SO_4. The solubility of ethanol in water is also shown, as a dashed−dotted line, extrapolated down to these temperatures.[33] Note that ethanol is less soluble in 39 wt % H_2SO_4 than in water, as discussed below. The solid lines in Figure 2 are best fits to the data for 39, 59, and 66 wt % H_2SO_4, with the intercept constrained as discussed below. The 39 and 59 wt % H_2SO_4 data include both the uptake (open symbols) and equilibrium (solid symbols) data. The equilibrium experiment data are discussed in detail below.

The measurements of ethanol dissolution in cold, aqueous H_2SO_4 provide thermodynamic information about this process. From the slope of the lines in Figure 2, the enthalpy of solvation ($\Delta H°$) can be determined according to eqs 4−6.[6]

$$\log H^* = A + 1000B/T \tag{4}$$

$$A = \Delta S°/2.303R + \log M_{solv} \tag{5}$$

$$B = -\Delta H°/2.303R \tag{6}$$

where A and B are the intercept and slope, respectively, $\Delta S°$ is

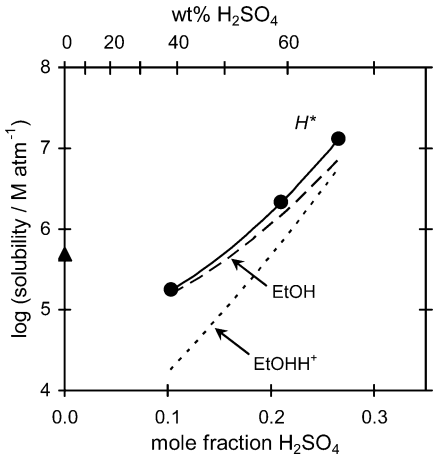

Figure 3. Solubility of ethanol in acidic solutions as a function of mole fraction H_2SO_4 at 220 K. The data are represented by solid circles (●), and the parameterization of the data is plotted as a solid black line. The fractions of this total solubility due to molecular and protonated ethanol as calculated from the pK_a[26,35] are also shown, as dashed and dotted lines, respectively. The solubility of ethanol in water at 220 K is plotted as a triangle, ▲.

the entropy of solvation, and M_{solv} is the molarity of water in the solutions, calculated at 220 K.[34] The thermodynamic parameters are reported in Table 2, with values from unconstrained best fits to the data shown in the top rows. Since large changes in the dissolution entropy of ethanol in H_2SO_4 relative to water are not expected and the uncertainty in $\Delta S°$ determined this way is substantial, we have fixed the value of $\Delta S°$ equal to that for ethanol dissolution in water, -174 J mol^{-1} K^{-1}.[33] The enthalpies of dissolution calculated by fixing $\Delta S°$ are also given in Table 2. The data for 59 wt % H_2SO_4 exhibit an unconstrained $\Delta S°$ very close to the value for water. For the 39 and 66 wt % acids, the difference this fixed entropy value makes in the calculated enthalpy of dissolution is more pronounced, 10% and 30%, respectively. A significantly more negative entropy of dissolution in the most dilute acid studied has also been observed for methanol[7] and acetaldehyde.[9] It is not yet clear whether this observation is meaningful or merely an artifact of the restricted temperature range accessible for the more dilute solutions in our experimental setup.

To determine the solubility of ethanol (eq 4) at conditions other than those studied herein, A can be calculated from eq 5 with $\Delta S° = -174$ J mol^{-1} K^{-1} and B can be calculated from the following empirical relation

$$B = 5.319*(x_{H_2SO_4})^2 + 0.812*(x_{H_2SO_4}) + 2.647 \qquad (7)$$

where $x_{H_2SO_4}$ is the mole fraction of sulfuric acid in the solution. Equation 7 is a polynomial fit to the experimental Henry's law coefficients at 220 K (the solid lines in Figure 2). This parameterization of ethanol solubility is plotted vs acid composition as a solid line in Figure 3; the experimentally measured solubility values are shown as black circles. Care must be taken not to extrapolate outside the experimental conditions with regard to acid composition (i.e., 39−66 wt % H_2SO_4 or 0.10−0.27 mole fraction H_2SO_4). The data for the 76 wt % acid are not included because they are too uncertain. Ethanol solubility in water[33] (shown as ▲ in Figure 3) has not been included in the parameterization because the minimum in solubility is not clearly defined by our data.

Henry's law solubility was also measured via the equilibrium vapor pressure of ethanol over ternary solutions. These results are reported in Table 3 and are plotted in Figure 2 as closed

TABLE 3: Measured Effective Henry's Law Coefficients for Equilibrium Vapor Pressure of Ethanol over Mixed Solutions

initial H_2SO_4/H_2O composition	[EtOH] (M)	T (K)	P_{EtOH} (atm)	$H*$ (M atm^{-1})
59.1 wt % H_2SO_4	0.5 M	214.3	1.3×10^{-7}	4.0×10^6
		224.0	4.5×10^{-7}	1.1×10^6
		230.8	1.2×10^{-6}	4.3×10^5
38.5 wt % H_2SO_4	0.1 M	214.0	3.0×10^{-7}	3.3×10^5
		219.4	5.8×10^{-7}	1.7×10^5
		223.9	1.1×10^{-6}	9.1×10^4

symbols: ■ for 39 wt % and ● for 59 wt % H_2SO_4. For the two ternary solutions 59 wt % acid, 0.5 M EtOH, and 39 wt % acid, 0.1 M EtOH, the determination of $H*$ with this method matched the results of the uptake experiments within experimental scatter. These data confirm the use of calculated diffusion coefficients and are therefore included in the parameterization reported in eq 7.

The data for the equilibrium experiments in the 66 wt % acid, 0.8 M EtOH solution, however, differed significantly from those of the uptake experiments. These data are plotted in Figure 2 as crosses (×); a best-fit line through the data is meant to guide the eye. The discrepancy between these data and the uptake data for 66 wt % H_2SO_4 is probably due to the large solution-phase concentration of ethanol (0.8 M), which is arguably not in the Henry's law regime. Furthermore, ethanol reduces the acidity of the solution. While we believe the data to be real, they are certainly not indicative of ethanol solubility in a pristine 66 wt % H_2SO_4 aqueous solution, and so no $H*$ values are reported for these experiments. While it is true that the 0.5 M ethanol in the ternary 59 wt % solution will also reduce acidity, the effect was not pronounced enough to distinguish from the uptake experiments. We cannot account for the difference in behavior between these two ternary solutions by errors in the values of D or otherwise. This behavior may be an indication of the extreme nonideality of sulfuric acid solutions.

The uncertainty in $H*$ is much larger in the most concentrated sulfuric acid solution (76 wt % H_2SO_4) uptake experiments than in the more dilute acids; variability between individual results at similar conditions was greater than an order of magnitude. Identifying the true slope from each $1/\gamma$ plot was difficult, since the slope was close to zero (i.e., a line with a slope of 0.01 fit the data as well as one with a slope of 0.001). This result demonstrates the limit of the experimental technique, which is ideal for solutes of lower solubility. For this reason, we show only the lower limits for the 76 wt % uptake data, plotted as pluses (+) in Figure 2, with a dotted line as an approximation of the lower limit. Thus, $H*$ for ethanol dissolution in 76 wt % H_2SO_4 is at least 10^7 M atm^{-1} under our experimental conditions but may be as high as 10^{10} M atm^{-1} below 230 K.

From Figure 3, it is clear that the amount of ethanol dissolution varies with acidity in the following way. As the acidity of the solution increases from pure water to pure acid, the solubility of ethanol decreases, passes through a minimum somewhere between 0 and 50 wt % H_2SO_4, and then increases sharply. Similar behavior has been observed for OVOCs such as acetaldehyde[9] and 2,4-pentanedione[36] and even simple hydrocarbons.[37,38] The increased solubility of oxygenated organics at higher acidity has often been attributed to the protonation of the oxygen atom(s) allowing more gas to be taken up into solution.[3,6,7] We can calculate the ratio of protonated ethanol ($EtOHH^+$) to molecular ethanol as a function of acid composition according to the excess acidity method[35]

$$\log \frac{[\mathrm{EtOHH^+}]}{[\mathrm{EtOH}]} = \log[\mathrm{H^+}] + \mathrm{p}K_a + m^*X \qquad (8)$$

where the H^+ concentration and excess acidity function X for aqueous H_2SO_4 solutions are from Cox.[35] This treatment of strongly acidic solutions depends on two variables: the excess acidity, X, and the slope factor, m^*. X is defined as the log of the ratio of activity coefficients for a theoretical reference base B*, $\log(\gamma_{B^*}\gamma_{H^+}/\gamma_{B^*H^+})$, and is a measure of how much more acidic the solution is than the stoichiometric acidity. The slope factor m^* is constant for a class of compounds and is associated with the hydrogen bonding of the solvent to the protonated base.[39] The experimentally measured pK_a of protonated ethanol is -2.12, and the slope factor, m^*, for alcohols is 0.17.[26] Our data describe the total solubility which we apportion to the two dissolved species based on their ratio calculated by eq 8. The resulting contributions to the overall solubility of ethanol from the molecular (EtOH, dashed line) and protonated ($EtOHH^+$, dotted line) forms are plotted in Figure 3. The excess acidity function and proton concentration have been adjusted to 220 K using the density of aqueous H_2SO_4 solutions.[34] Unfortunately, the protonation enthalpy of ethanol in sulfuric acid has not been measured or calculated to our knowledge, and so the room-temperature pK_a was used. In this case, the molecular and protonated forms are equal in concentration at just under 70 wt % H_2SO_4, and the molecular form of ethanol is dominant over the range of the solubility parameterization. The protonated form does, however, contribute 10−44% of total dissolved ethanol from 39 to 66 wt % H_2SO_4. (If the protonation enthalpy were $+10$ kJ mol^{-1}, then this crossing point would change to ∼50 wt % at 220 K, meaning the protonated form would dominate for most of our solutions. Conversely, if it were -10 kJ mol^{-1}, then the crossing point would change to ∼80 wt % at 220 K. The protonation enthalpy has been measured for aldehydes and ketones and ranges from $+2$ kJ mol^{-1} for benzaldehyde to -56 kJ mol^{-1} for methyl benzoate,[39] so it seems likely that molecular ethanol was the primary dissolved species in our experiments.)

According to our measurements and the excess acidity method, the solubility of molecular ethanol (i.e., unprotonated) increases with acidity by a factor of 36 from 39 wt % to 66 wt % H_2SO_4. A reasonable comparison can be made to cyclopentane, which presumably is not protonated by acid as oxygenated compounds are. Cyclopentane is more soluble in pure sulfuric acid than in water, but at 75 wt % H_2SO_4, its solubility is only two-thirds that of its solubility in water.[38] In contrast, at only 66 wt % H_2SO_4, molecular ethanol is 14 times more soluble than in water. Figure 3 indicates that protonation is not the sole, or even primary, reason for increasing overall solubility of gaseous ethanol with acidity. In fact, sulfuric acid is a much better solvent for ethanol than is pure water. Traditionally, a Setchnow coefficient has been used to describe the decreasing dissolution of gases in solutions of high ionic strength.[16,40] While this approach may be valid for inorganic acids in sulfuric acid, we confirm that it is clearly not appropriate for OVOCs in sulfuric acid[41] which exhibit large increases in solubility, regardless of protonation, as acidity increases.

Once dissolved, ethanol may react in cold sulfuric acid under UT/LS conditions. At room temperature, the formation of ethyl hydrogen sulfate (esterification) is documented[42,43]

$$\mathrm{CH_3CH_2OH + H_2SO_4 \rightleftarrows CH_3CH_2OSO_3H + H_2O} \qquad (9)$$

Unfortunately, the ethyl hydrogen sulfate product of this reaction is not volatile and thus is undetectable in our system. However, solution-phase reaction can be observed in the time dependence of the uptake coefficient.[25] For a fast reaction, uptake is constant. If, however, loss due to reaction is comparable to diffusion into the bulk, then the $1/\gamma$ vs $t^{1/2}$ plot will curve downward (i.e., uptake is higher than for simple dissolution), as has been observed under some conditions for acetaldehyde uptake by sulfuric acid.[9] No such behavior was observed for ethanol uptake by H_2SO_4.

This reaction is slow even at room temperature (the lifetime of ethanol is 4 h in 76 wt % H_2SO_4 and 4 years in 39 wt % H_2SO_4)[42,43] and the exposure of acid to ethanol in our experiments is short (2 to 20 min). Therefore, the ternary solution of 59 wt % H_2SO_4, 0.5 M EtOH was stored at 250 K for 40 days to allow sufficient time for reaction. The equilibrium vapor pressure of ethanol over the aged solution was then remeasured in the Knudsen cell at 231 K. Initially, the ethanol pressure over the solution was 0.88 mTorr (1.2×10^{-6} atm); after 40 days at 250 K, it had decreased to 0.76 mTorr (1.0×10^{-6} atm). This pressure difference could indicate a 14% conversion of ethanol to product. However, this pressure change is well within our experimental uncertainty and therefore is not proof of reaction. If due to reaction, then it corresponds to an upper bound on the first-order rate constant, $k \leq 1 \times 10^{-6}$ s^{-1}, which is slightly below the room-temperature rate constant of 1.3×10^{-6} s^{-1} from Deno and Newman[42] assuming the same acidity dependence as methanol. An upper bound on the rate constant can also be determined by fitting the uptake data to eq 2. There are three unknowns: the intercept ($1/\Gamma_g + 1/\alpha$), H^*, and k. The first two variables were kept constant, and k was varied to find the maximum value where eq 2 still fell within the range of experimental values. Determined this way, the upper bound for k is 3×10^{-6} s^{-1} for 59 wt % H_2SO_4. A similar analysis of methanol uptake by 45 wt % H_2SO_4 found $k \leq 3 \times 10^{-5}$ s^{-1} for the slightly faster methanol esterification reaction.[7]

IV. Conclusions and Implications

The solubility of gas-phase ethanol in aqueous sulfuric acid solutions was measured over ranges of temperature (209−237 K) and acid composition (39−76 wt % H_2SO_4). The effective Henry's law coefficient ranges from 4×10^4 M atm^{-1} in the 227 K, 39 wt % acid to greater than 10^7 M atm^{-1} in the 76 wt % acid. While protonation does increase the solubility of ethanol, a large increase of molecular ethanol in solution (or a large positive protonation enthalpy for ethanol) is necessary to account for the measured solubility reported herein. If ethyl hydrogen sulfate is formed under our experimental conditions, then the first-order rate constant is no higher than $\sim 1 \times 10^{-6}$ s^{-1}.

The high solubility of ethanol means that even though it is a minor trace gas in the atmosphere, it may be a major trace constituent in particles. The equilibrium organic content for a typical UT sulfate particle (0.1 μm radius, 220 K, 58 wt % H_2SO_4, 12 km, 160 Torr) calculated from the background mixing ratios of oxygenated organic compounds as reported by Singh et al.[1] and their measured solubilities[6,7,9,44] under these conditions is as follows. For 800 pptv of methanol,[7] 70 pptv of ethanol (this work), 600 pptv of acetone,[6] 50 pptv of formaldehyde,[44] and 80 pptv of acetaldehyde,[9] we find that ethanol is responsible for almost a quarter of the particle organic content by mass, even though its gas-phase mixing ratio is among the lowest. The organic mass fraction due to the dissolution of these five gases is less than 0.001% of the particle mass. Simple solubility cannot, therefore, account for organic matter detected in UT/LS particles by Murphy et al.,[2] which is significantly higher than their reported detection limit of ∼0.02 wt % organic matter (α-tocopherol).[45] If the equilibrium amount of dissolved ethanol

in this typical particle is allowed to react for 10 days at the upper limit of the rate constant, some ethyl hydrogen sulfate is formed (~200 molecules per particle). Nevertheless, this amount does not increase the organic mass content above 0.001%. Since the esterification of alcohols is not fast enough to be atmospherically significant, other reaction pathways may be responsible for the accumulation of organic matter in sulfate particles and are under investigation in our laboratory.

Acknowledgments. This work was performed while R.R.M. held a National Research Council Associateship Award at NASA Ames Research Center. S.J.R.S. was supported by the NASA Undergraduate Student Research Program. This work was funded by the NASA Upper Atmosphere Research and New Investigator Programs. The authors thank G. Nathanson, D. Golden, R. Walsh, J. Elsila, R. Chatfield, and T. Huthwelker for helpful comments.

Supporting Information Available: The data in Tables 1−3 and eq 7 have been adjusted for the maximum possible correction due to thermal transpiration as discussed in the Experimental Methods section. This material is available free of charge via the Internet at http://pubs.acs.org.

References and Notes

(1) Singh, H. B.; Salas, L. J.; Chatfield, R. B.; Czech, E.; Fried, A.; Walega, J.; Evans, M. J.; Field, B. D.; Jacob, D. J.; Blake, D.; Heikes, B.; Talbot, R.; Sachse, G.; Crawford, J. H.; Avery, M. A.; Sandholm, S.; Fuelberg, H. *J. Geophys. Res.* **2004**, *109*, 15S07.

(2) Murphy, D. M.; Thompson, D. S.; Mahoney, M. J. *Science* **1998**, *282*, 1664.

(3) Duncan, J. L.; Schindler, L. R.; Roberts, J. T. *J. Phys. Chem. B* **1999**, *103*, 7247.

(4) Imamura, T.; Akiyoshi, H. *Geophys. Res. Lett.* **2000**, *27*, 1419.

(5) Kane, S. M.; Timonen, R. S.; Leu, M. T. *J. Phys. Chem. A* **1999**, *103*, 9259.

(6) Klassen, J. K.; Lynton, J.; Golden, D. M.; Williams, L. R. *J. Geophys. Res.* **1999**, *104*, 26355.

(7) Iraci, L. T.; Essin, A. M.; Golden, D. M. *J. Phys. Chem. A* **2002**, *106*, 4054.

(8) Kane, S. M.; Leu, M. T. *J. Phys. Chem. A* **2001**, *105*, 1411.

(9) Michelsen, R. R.; Ashbourn, S. F. M.; Iraci, L. T. *J. Geophys. Res.* **2004**, *109*, 23205.

(10) DeMott, P. J.; Cziczo, D. J.; Prenni, A. J.; Murphy, D. M.; Kreidenweis, S. M.; Thomson, D. S.; Borys, R.; Rogers, D. C. *Proc. Natl. Acad. Sci. U.S.A.* **2003**, *100*, 14655.

(11) Kanakidou, M.; David, P.; Poisson, N. Impact of VOCs of natural and anthropogenic origin on the oxidizing capacity of the atmosphere. In *Transport and Chemical Transformation of Pollutants in the Troposphere*; Ebel, A., Friedich, R., Rodhe, H., Eds.; Springer: Berlin, 1997; p 392.

(12) Poulopoulos, S. G.; Samaras, D. P.; Philippopoulos, C. *Atmos. Environ.* **2001**, *35*, 4399.

(13) Colón, M.; Pleil, J. D.; Hartlage, T. A.; Guardani, M. L.; Martins, M. H. *Atmos. Environ.* **2001**, *35*, 4017.

(14) Nguyen, H. T. H.; Takenaka, N.; Bandow, H.; Maeda, Y.; de Olivia, S. T.; Botelho, M. M. F.; Tavares, T. M. *Atmos. Environ.* **2001**, *35*, 3075.

(15) Hess, G. *Chem. Eng. News* **2005**, *83*, 12.

(16) Sander, S. P.; Friedl, R. R.; Ravishankara, A. R.; Golden, D. M.; Kolb, C. E.; Kurylo, M. J.; Huie, R. E.; Orkin, V. L.; Molina, M. J.; Moortgat, G. K.; Finlayson-Pitts, B. J. *Chemical Kinetics and Photochemical Data for Use in Atmospheric Studies*; Evaluation No. 14, JPL Publication 02-25; Jet Propulsion Laboratory: Pasedena, CA, 2003.

(17) Dickerson, R. R.; Huffman, G. J.; Luke, W. T.; Nunnermacker, L. J.; Pickering, K. E.; Leslie, A. C. D.; Lindsey, C. G.; Slinn, W. G. N.; Kelly, T. J.; Daum, P. H.; Delany, A. C.; Greenberg, J. P.; Zimmerman, P. R.; Boatman, J. F.; Ray, J. D.; Stedman, D. H. *Science* **1987**, *235*, 460.

(18) Thompson, A. M.; Tao, W.-K.; Pickering, K. E.; Scala, J. R.; Simpson, J. *Bull. Am. Meterol. Soc.* **1997**, *78*, 1043.

(19) Jost, H.-J.; Drdla, K.; Stohl, A.; Pfister, L.; Lowenstein, M.; Lopez, J. P.; Hudson, P. K.; Murphy, D. M.; Cziczo, D. J.; Fromm, M.; Bui, T. P.; Dean-Day, J.; Gerbig, C.; Mahoney, M. J.; Richard, E. C.; Spichtinger, N.; Pittman, J. V.; Weinstock, E. M.; Wilson, J. C.; Xueref, I. *Geophys. Res. Lett.* **2004**, *31*, L11101.

(20) Fischer, H.; de Reus, M.; Traub, M.; Williams, J.; Lelieveld, J.; de Gouw, J.; Warneke, C.; Schlager, H.; Minikin, A.; Scheele, R.; Siegmund, P. *Atmos. Chem. Phys.* **2003**, *3*, 739.

(21) Golden, D. M.; Spokes, G. N.; Benson, S. W. *Angew. Chem.* **1973**, *12*, 534.

(22) Brimblecombe, P.; Clegg, S. L.; Wexler, A. S. Aerosol Inorganics Model. http://www.uea.ac.uk/~e770/aim.html (accessed July 2004).

(23) Carslaw, K. S.; Clegg, S. L.; Brimblecombe, P. *J. Phys. Chem.* **1995**, *99*, 11557.

(24) Massucci, M.; Clegg, S. L.; Brimblecombe, P. *J. Phys. Chem. A* **1999**, *103*, 4209.

(25) Finlayson-Pitts, B. J.; Pitts, J. N. *Chemistry of the Upper and Lower Atmosphere*; Academic Press: San Diego, CA, 2000.

(26) Lee, D. G.; Demchuk, K. J. *Can. J. Chem.* **1987**, *65*, 1769.

(27) Reid, R. C.; Prausnitz, J. M.; Poling, B. E. *The Properties of Gases and Liquids*, 4th ed.; McGraw-Hill Book Co.: New York, 1987.

(28) Williams, L. R.; Long, F. S. *J. Phys. Chem.* **1995**, *99*, 3748.

(29) Kennard, E. H. *Kinetic Theory of Gases*; McGraw-Hill Book Company, Inc.: New York, 1938.

(30) Poulter, K. F.; Rodgers, M.-J.; Nash, P. J.; Thompson, T. J.; Perkin, M. *Vacuum* **1983**, *33*, 311.

(31) Růžička, K.; Fulem, M.; Růžička, V. *J. Chem. Eng. Data* **2005**, *50*, 1956.

(32) Dankwerts, P. V. *Gas−Liquid Reactions*; McGraw-Hill Book Company: New York, 1970.

(33) Snider, J. R.; Dawson, G. A. *J. Geophys. Res.* **1985**, *90*, 3797.

(34) Myhre, C. E. L.; Christensen, D. H.; Nicolaisen, F. M.; Nielsen, C. J. *J. Phys. Chem. A* **2003**, *107*, 1979.

(35) Cox, R. A. *Adv. Phys. Org. Chem.* **2000**, *35*, 1.

(36) Nozière, B.; Riemer, D. D. *Atmos. Environ.* **2003**, *37*, 841.

(37) Rudakov, E. S.; Lutsyk, A. I. *Russ. J. Phys. Chem.* **1979**, *53*, 731.

(38) Rudakov, E. S.; Lutsyk, A. I.; Suikov, S. Y. *Russ. J. Phys. Chem.* **1987**, *61*, 601.

(39) Bagno, A.; Lucchini, V.; Scorrano, G. *J. Phys. Chem.* **1991**, *95*, 345.

(40) Jayne, J. T.; Worsnop, D. R.; Kolb, C. E.; Swartz, E.; Davidovits, P. *J. Phys. Chem.* **1996**, *100*, 8015.

(41) Sanders, S. J. *Ind. Eng. Chem. Process Des. Dev.* **1985**, *24*, 942.

(42) Deno, N. C.; Newman, M. S. *J. Am. Chem. Soc.* **1950**, *72*, 3852.

(43) Clark, D. J.; Williams, G. *J. Chem. Soc.* **1957**, 4218.

(44) Iraci, L. T.; Tolbert, M. A. *J. Geophys. Res.* **1997**, *102*, 16099.

(45) Middlebrook, A. M.; Thomson, D. S.; Murphy, D. M. *Aerosol. Sci. Technol.* **1997**, *27*, 293.